Engineering xxx (xxxx) xxx

Contents lists available at ScienceDirect

Engineering

journal homepage: www.elsevier.com/locate/eng

Research
Microecology—Article

Pien Tze Huang Protects Against Non-Alcoholic Steatohepatitis by Modulating the Gut Microbiota and Metabolites in Mice

Xianyi Zeng [a,#], Xiang Zhang [a,b,#], Hao Su [a], Hongyan Gou [a], Harry Cheuk-Hay Lau [b], Xiaoxu Hu [a], Ziheng Huang [a], Yan Li [a], Jun Yu [a,b,*]

[a] *Shenzhen Research Institute, The Chinese University of Hong Kong, Shenzhen 518057, China*
[b] *Department of Medicine and Therapeutics, Institute of Digestive Disease, State Key Laboratory of Digestive Disease, Li Ka Shing Institute of Health Sciences, The Chinese University of Hong Kong, Hong Kong 999077, China*

ARTICLE INFO

Article history:
Received 15 May 2022
Revised 15 October 2022
Accepted 30 October 2022
Available online xxxx

Keywords:
Pien Tze Huang
Non-alcoholic steatohepatitis
Gut barrier function
Gut microbiota

ABSTRACT

Non-alcoholic steatohepatitis (NASH) is a severe form of non-alcoholic fatty liver disease without effective treatment. The traditional Chinese medicine formulation Pien Tze Huang (PTH) can suppress inflammatory diseases. Here, we evaluate the effects of PTH on the evolution of NASH and its underlying mechanisms. We found that PTH prevented the development of steatohepatitis induced by various dietary models, including a high-fat high-cholesterol (HFHC) diet, choline-deficient high-fat diet (CD-HFD), and methionine- and choline-deficient (MCD) diet, along with significant suppression of liver injury, hepatic triglyceride, and lipid peroxidation. Moreover, ten days of PTH treatment after the onset of NASH significantly ameliorated MCD diet-induced steatosis and liver injury in mice. Through the metagenomic sequencing of stool samples, we found that PTH administration restored the gut microbiota with enrichment of probiotics including *Lactobacillus acidophilus* (*L. acidophilus*), *Lactobacillus plantarum*, *Lactococcus lactis*, and *Bacillus subtilis*. The enriched *L. acidophilus* prevented MCD diet-induced steatohepatitis. In addition, PTH restored the gut barrier function in mice with steatohepatitis, as evidenced by reduced intestinal permeability, decreased serum lipopolysaccharides (LPS) level, and increased epithelial tight-junction protein E-cadherin expression. Our metabolomic analysis via liquid chromatography-mass spectrometry profiling identified the alteration in the metabolism of bile acids in the portal vein of PTH-treated mice. We further confirmed that an intact gut microbiota is necessary for PTH to exhibit anti-steatohepatitis effects. In conclusion, PTH protects against steatohepatitis development by modulating the gut microbiota and metabolites. PTH is a potential promising prophylactic and therapeutic option for patients with NASH.

1. Introduction

Non-alcoholic fatty liver disease (NAFLD) is a major cause of morbidity and a healthcare burden worldwide, affecting 25% of the global adult population and 34% of the Asian population [1]. About 20% of NAFLD patients progress to non-alcoholic steatohepatitis (NASH), which is a severe stage of NAFLD with hepatocyte injury, liver inflammation, and/or pericellular fibrosis [2]. Although several supplements and drugs such as vitamin E, peroxisome proliferator-activated receptor agonist, and pentoxifylline have borderline efficacy in NASH therapy, they are restricted in clinical use due to their potential side effects and toxicity [3,4]. As a result, no drug has been approved to date by the US Food and Drug Administration or the National Medical Products Administration for NASH therapy. Identifying safe and effective therapeutics against NASH is an unmet clinical need.

Traditional Chinese medicine (TCM) is known for its advantages in terms of its multi-target and multi-channel mechanisms of action [5]. Pien Tze Huang (PTH) is a TCM formula that is widely used in China and Southeast Asia for treating viral hepatitis and inflammatory diseases [6]. It is composed of four TCM ingredients: *Radix et Rhizoma Notoginseng* (85%), *Moschus* (3%), *Calculus Bovis* (5%), and snake gallbladder (7%). The effect of PTH in the treatment of NASH has not been investigated.

* Corresponding author.
E-mail address: junyu@cuhk.edu.hk (J. Yu).
# These authors contributed equally to this work.

https://doi.org/10.1016/j.eng.2022.10.010

Please cite this article as: X. Zeng, X. Zhang, H. Su et al., Pien Tze Huang Protects Against Non-Alcoholic Steatohepatitis by Modulating the Gut Microbiota and Metabolites in Mice, Engineering, https://doi.org/10.1016/j.eng.2022.10.010

Different dietary NASH models that recapitulate human NASH have been developed [7]. The methionine- and choline-deficient (MCD) diet replicates NASH histological phenotypes (i.e., severe inflammation, steatosis, oxidative stress, and fibrosis) within a shorter duration than other dietary models of NASH. However, the MCD diet can cause weight loss and does not induce features of metabolic syndrome in NASH [7]. In comparison, although a relatively long duration is needed for mice to develop NASH induced by a choline-deficient high-fat diet (CD-HFD), key features of human metabolic syndrome and NASH are mimicked in this model [8]. However, the CD-HFD is a diet-deficient model that cannot mimic an actual human diet. The high-fat high-cholesterol (HFHC) diet model is a Western diet model that has been well established by our research team [9]. It mirrors various phenotypes of NASH and their associated metabolic changes, including lipid accumulation, inflammation, oxidative stress, liver injury, obesity, and insulin resistance. Moreover, the HFHC diet induces gut microbiome dysbiosis and metabolites alteration, further contributing to NASH progression [9,10].

Recent studies have demonstrated the crucial role of the gut microbiota in NASH progression [9,11]. Gut microbial dysbiosis and its associated metabolites, such as bile acids, trimethylamine, and short-chain fatty acids (SCFAs), contribute to NASH initiation and progression [12]. Given the importance of microbes and their metabolites, the therapeutic potential of modulating the gut microbiota to protect against liver diseases has been suggested. In particular, TCM has long been acknowledged for its ability to alter the gut microbiota to confer health benefits. TCM was reported to ameliorate metabolic syndrome by modulating the gut microbiota [13] and improving lipid metabolism by regulating metabolites including SCFAs and bile acids [14]. As NASH is a complex multifactorial disease, TCM may have therapeutic potential in NASH by targeting both the gut microbiota and host physiology. In this study, we investigated the role of PTH in the prevention and treatment of NASH using multiple dietary mouse models. The contribution of the gut microbiota and metabolites and the change of gut barrier function in experimental NASH with or without PTH treatment were also elucidated.

2. Materials and methods

2.1. Mice and treatments

Male C57BL/6 mice (6–7 weeks old) were randomly assigned to be fed with normal chow (NC), an HFHC diet with 23 $g{\cdot}L^{-1}$ of fructose supplemented in drinking water [15] for 12 weeks or a CD-HFD (Specialty Feeds Pty. Ltd., Australia) for 20 weeks (n = 8–10 per group). NASH was also induced in another model by feeding male C57BL/6 mice (6–7 weeks old) with an MCD diet or the corresponding control diet (Specialty Feeds Pty. Ltd.) for 5 days, 10 days, or 4 weeks, respectively (n = 8–10 per group). Mice were gavaged with PTH (540 $mg{\cdot}kg^{-1}$; Zhangzhou Pien Tze Huang Pharmaceutical Co., Ltd., China) or phosphate-buffered saline (PBS) every day. At the experimental end points, the mice were fasted and serum/tissues were harvested. Body weights and visceral fat weights were recorded. Liver tissues were rapidly excised and weighed. Fecal samples and portal vein blood were collected for metagenomic sequencing and metabolomic profiling, respectively.

In an additional experiment, male C57BL/6 mice (6–7 weeks old) were treated with an antibiotics cocktail to verify the role of the microbiota in PTH-suppressed NASH. Drinking water was supplemented with an antibiotics cocktail (0.2 $g{\cdot}L^{-1}$ of ampicillin, 0.2 $g{\cdot}L^{-1}$ of neomycin, 0.2 $g{\cdot}L^{-1}$ of metronidazole, and 0.1 $g{\cdot}L^{-1}$ of vancomycin) for 2 weeks, every other 2 weeks until the end of the experiment, to deplete the gut microbiota [16]. Mice were harvested 12 weeks after HFHC diet feeding as well as 4 weeks after MCD diet treatment.

In order to explore the role of probiotics in PTH-ameliorated NASH, male C57BL/6 mice (6–7 weeks old) were fed with an MCD diet and gavaged with *L. acidophilus* (1×10^9 colony-forming unit (CFU) per 200 μL per day), *Escherichia coli* (*E. coli*) strain MG1655 (bacteria control), or PBS for 10 consecutive days. All the mice were maintained in a specific-pathogen-free environment with controlled conditions: namely, a 12-h light/dark cycle at 20–22 °C and (45 ± 5)% humidity. All procedures adhered to the guidelines approved by the Animal Experimentation Ethics Committee of The Hong Kong Polytechnic University Shenzhen Research Institution (IACUC No.: 181105).

2.2. Shotgun metagenomic sequencing and analysis

To determine PTH-induced gut microbiota alterations, DNA was extracted from fecal samples using a QIAamp DNA mini kit (QIAGEN, Germany). Shotgun metagenomic sequencing of mice fecal DNA was performed on an Illumina HiSeq 2000 platform (Illumina, USA). Raw sequence reads were first trimmed using Trimmomatic (version 0.39) to remove low-quality reads and adaptors. The trimmed reads were aligned with Bowtie2 (version 2.4.4) against the host (mouse mm10) genome to remove human reads with the "very sensitive" default parameter settings. Kraken2 (version 2.0.8) was then used for taxonomy classification of the unmapped reads (Table S1 in Appendix A). Bracken was used to produce accurate species-level abundance estimates with the results of Kraken2. Diversity richness (Chao1 index) was calculated by means of *R* package phyloseq and vegan. Visualization of the microbiota between different groups was based on the Bray–Curtis dissimilarity matrix. We used Ebseq for the differential analyses of metagenomic data. We used the ternary plot method to identify bacteria associated with PTH treatment at the genus level.

2.3. Metabolomic profiling and analysis

Liquid chromatography-mass spectrometry (LC-MS) analyses were performed using an ultra-high-performance liquid chromatography (UPLC) system (1290; Agilent Technologies, USA) with a Waters UPLC BEH C18 column (1.7 μm, 2.1 mm × 100 mm; USA) from Shanghai Biotree Biotech. The column temperature was set at 55 °C and the sample injection volume was set at 5 μL. The flow rate was set at 0.5 $mL{\cdot}min^{-1}$.

The mobile phase consisted of 0.1% formic acid in water and 0.1% formic acid in acetonitrile. The multistep linear elution gradient program was as follows: 0–11.0 min, 85%–25% A; 11.0–12.0 min, 25%–2% A; 12.0–14.0 min, 2%–2% A; 14.0–14.1 min, 2%–85% A; 14.1–15.0 min, 85%–85% A; 15–16 min, 85%–85% A. A Q Exactive Focus mass spectrometer (Thermo Fisher Scientific, Finland) coupled with Xcalibur software was employed to obtain the mass spectrometry (MS) and tandem mass spectrometry (MS/MS) data based on the information-dependent acquisition mode. During each acquisition cycle, the mass range was from 100 to 1500. The top three masses of every cycle were screened, and the corresponding MS/MS data were further acquired. The sheath gas flow rate was 45 arbitrary units (Arb), the aux gas flow rate was 15 Arb, the capillary temperature was 400 °C, the full MS resolution was 70 000, the MS/MS resolution was 17 500, the collision energy was 15/30/45 in normalized collision energy (NCE) mode, and the spray voltage was 4.0 kV (positive) or −3.6 kV (negative). An in-house MS2 database was applied for metabolites identification. Limma was used for the differential analyses of metabolomics profiling data. The Benjamini–Hochberg method was used to control the false discovery rate (FDR). FDR < 0.01 and abs(log(fold change)) > 2 were considered as significant different. Clustering analysis was performed based on the results of screening out different metabolites.

2.4. Biochemical assay

Serum was obtained by centrifuging whole blood samples. The levels of serum alanine aminotransferase (ALT), aspartate aminotransferase (AST), cholesterol, and triglyceride were determined using a Catalyst One Chemistry Analyzer (IDEXX Laboratories, USA). Total cholesterol (JL13847-48 T) and triglycerides (JL13528-48 T) in mice livers were measured by means of corresponding assay kits (Shanghai Jianglai Biotechnology Co., Ltd., China). Lipid peroxidation was quantified by measuring malondialdehyde using a thiobarbituric acid reactive substances (TBARs) assay (Shanghai Jianglai Biotechnology Co., Ltd.).

2.5. Histological analysis

Liver histology was assessed via hematoxylin and eosin (H&E) staining of paraffin-embedded sections. Two pathologists who were blinded to the treatment evaluated the stained slides independently and assigned scores for steatosis and inflammation. Steatosis was scored via a low-to-medium power evaluation of parenchymal involvement according to the following criteria: 0 (< 5%), 1 (5%–33%), 2 (33%–66%), or 3 (> 66%). Inflammation was scored by an overall assessment of all inflammatory foci according to the following criteria: 0 (no foci), 1 (< 2 foci per 200X field), 2 (2–4 foci per 200X field), or 3 (> 4 foci per 200X field). Oil Red O staining was performed on optimal cutting temperature compound-embedded frozen liver sections.

2.6. Measurement of pro-inflammatory cytokines

Serum tumor necrosis factor α (TNFα) and interleukin-6 (IL-6) levels were measured using a mouse TNFα enzyme-linked immunosorbent assay (ELISA) kit and mouse IL-6 ELISA kit (Shanghai Jianglai Biotechnology Co., Ltd.), according to the manufacturer's instructions.

2.7. Quantitative real-time polymerase chain reaction (qRT-PCR)

The total RNA was extracted from mouse liver using TRIzol Reagent (Thermo Fisher Scientific). RNA quality was determined using a spectrophotometer and was reversely transcribed using a complementary DNA conversion kit (Thermo Fisher Scientific). Fecal bacterial DNA was extracted using a QIAamp DNA mini kit. Liver complementary DNA (cDNA) and bacterial DNA were used for a qRT-PCR using SYBR Green Master Mix (Roche, Switzerland) in a Light Cycler 480 real-time PCR system (Roche). The primers used are listed in Table S2 in Appendix A.

2.8. Intestinal permeability assay

A 100 $mg \cdot mL^{-1}$ solution of fluorescein isothiocyanate (FITC)-dextran (Sigma-Aldrich, USA) was orally gavaged into each mouse (0.3 $mg \cdot g^{-1}$ body weight). Retro-orbital blood was collected 5 h after FITC-dextran administration and was maintained at 4 °C overnight. The blood was subsequently centrifuged at 3000 rotations per minute (rpm) for 20 min. The FITC-dextran in the serum was determined at excitation wavelength of 490 nm and emission wavelength of 530 nm [17].

2.9. Measurement of serum lipopolysaccharides

Serum was collected from portal vein of mice when harvesting. The serum lipopolysaccharide (LPS) level was measured using a mouse LPS enzyme-linked immune sorbent assay kit (Cusabio, China), according to the manufacturer's instructions.

2.10. Western blot test

The total protein in 30–50 mg of tissues was obtained using CytoBuster protein extraction reagent (Merch Chemicals, UK). Protein concentration was measured using a detergent compatible protein assay (BIO-RAD, USA). Protein (20–40 mg) was first separated by means of 5% upper gel and 10% lower gel, and then transferred onto polyvinylidene difluoride membranes (GE Healthcare, USA). Membranes were incubated first with E-cadherin primary antibody (Catalog No.: 14472; Cell Signaling Technology, USA) overnight at 4 °C and then with secondary antibody at room temperature for 1 h. E-cadherin protein was visualized using ECL Plus Western Blot Detection Reagents (GE Healthcare). β-actin was used as the total protein loading control.

2.11. Statistical analyses

Differences between the two groups were compared by means of Student's *t* test or a Mann–Whitney *U* test. Multiple group comparisons were assessed using a Kruskal–Wallis test or one-way analysis of variance (ANOVA). All statistical tests were performed using GraphPad Prism or *R* Software. Data were considered significant at $P < 0.05$.

3. Results

3.1. PTH prevents HFHC diet-induced steatohepatitis

To explore the effects of PTH on steatohepatitis, C57BL/6 mice were fed with an HFHC diet for 12 weeks to induce NASH development. Mice were administered with PTH or PBS control (Fig. 1(a)). HFHC diet-fed mice supplemented with PTH exhibited a lower body weight compared with HFHC diet-fed mice supplemented with the PBS control ($P < 0.01$) (Fig. 1(b)). Histological examination of liver sections showed that PTH treatment significantly improved liver histology with reduced liver steatosis ($P < 0.01$) and inflammatory cell infiltration ($P < 0.05$), compared with HFHC diet-fed mice without PTH supplementation (Fig. 1(c)). The decreased lipid accumulation in PTH-supplemented mice was confirmed by Oil Red O staining (Fig. 1(c)). Consistent with the histological findings, PTH decreased blood and hepatic lipids in mice, as evidenced by significantly reduced levels of triglyceride and total cholesterol ($P < 0.05$ for serum and hepatic triglyceride; $P < 0.001$ for serum and hepatic total cholesterol) (Fig. 1(d)). Measurements of hepatic lipid peroxide ($P < 0.01$) and serum ALT and AST (both $P < 0.05$) revealed that PTH significantly protected mice from HFHC diet-induced liver injury (Figs. 1(e) and (f)). Moreover, PTH significantly reduced the serum levels of key pro-inflammatory mediators in NASH including TNFα ($P < 0.01$) and IL-6 ($P < 0.001$) in HFHC diet-fed mice (Fig. 1(g)). Collectively, these results suggest that PTH acts as a prophylaxis against the development of steatohepatitis.

3.2. PTH prevents CD-HFD or MCD diet-induced steatohepatitis

To confirm the preventive effects of PTH, we established a second NASH mouse model induced by a CD-HFD. Mice were fed with a CD-HFD supplemented with PTH or PBS control for 12 weeks. Mice developed steatohepatitis after 20 weeks feeding with a CD-HFD (Fig. 2(a)). Consistent with the observations in HFHC diet-fed mice, CD-HFD-fed mice with PTH supplementation showed significantly decreased body weight, liver weight, and adipose tissue weight compared with CD-HFD-fed mice supplemented with the PBS control (all $P < 0.001$) (Fig. 2(b)). PTH

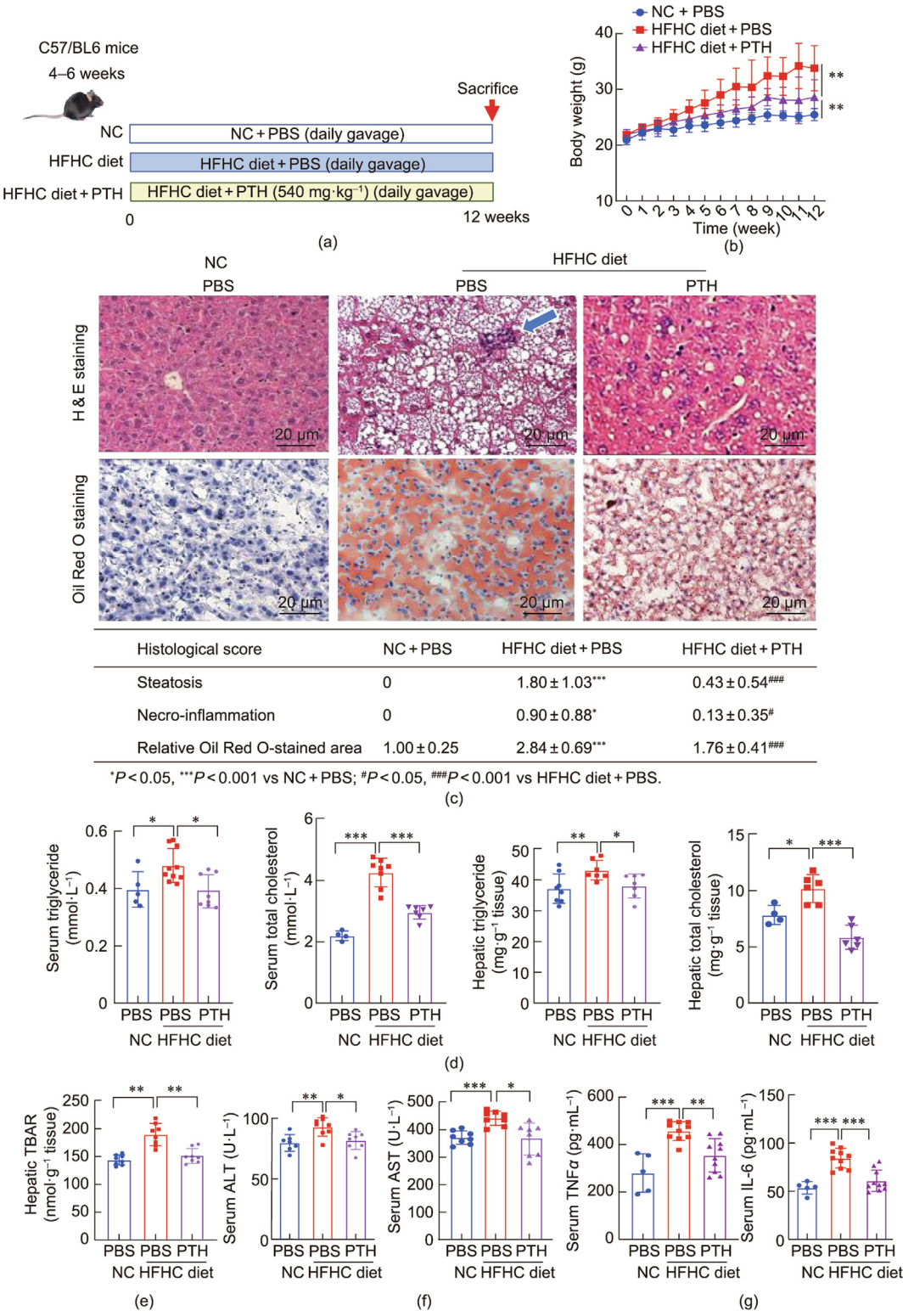

Histological score	NC + PBS	HFHC diet + PBS	HFHC diet + PTH
Steatosis	0	$1.80 \pm 1.03^{***}$	$0.43 \pm 0.54^{\#\#\#}$
Necro-inflammation	0	$0.90 \pm 0.88^{*}$	$0.13 \pm 0.35^{\#}$
Relative Oil Red O-stained area	1.00 ± 0.25	$2.84 \pm 0.69^{***}$	$1.76 \pm 0.41^{\#\#\#}$

(c) $^{*}P < 0.05$, $^{***}P < 0.001$ vs NC + PBS; $^{\#}P < 0.05$, $^{\#\#\#}P < 0.001$ vs HFHC diet + PBS.

Fig. 1. PTH prevents the development of HFHC diet-induced steatohepatitis. (a) Experimental design for mice fed with NC or an HFHC diet supplemented with PTH or PBS control. (b) The HFHC diet increased body weight, while PTH supplement decreased HFHC-induced body weight gain. (c) Representative H&E staining (the arrow indicates inflammatory cells) and Oil Red O staining from liver sections of mice fed with NC or an HFHC diet with or without PTH supplementation. Histological scores of steatosis and inflammation were determined. Quantification of the Oil Red O stained area was performed by Image J. The scale bar represents 20 μm. (d) Serum triglyceride, total cholesterol, hepatic triglyceride, and hepatic cholesterol levels; (e) hepatic TBARs; (f) serum ALT and AST levels; and (g) serum TNFα and IL-6 levels in mice fed with NC or an HFHC diet with or without PTH supplementation. $^{*}P < 0.05$, $^{**}P < 0.01$, $^{***}P < 0.001$.

administration also attenuated the development of steatohepatitis, with improved liver histology including significantly reduced steatosis ($P < 0.01$) and inflammation ($P < 0.001$) (Fig. 2(c)). Attenuated steatohepatitis due to PTH was confirmed by decreased levels of serum cholesterol, hepatic triglyceride, hepatic total cholesterol (Fig. 2(d)); liver lipid peroxidation (Fig. 2(e)); serum ALT levels (Fig. 2(f)); and pro-inflammatory cytokines TNFα and IL-6 (Fig. 2(g)).

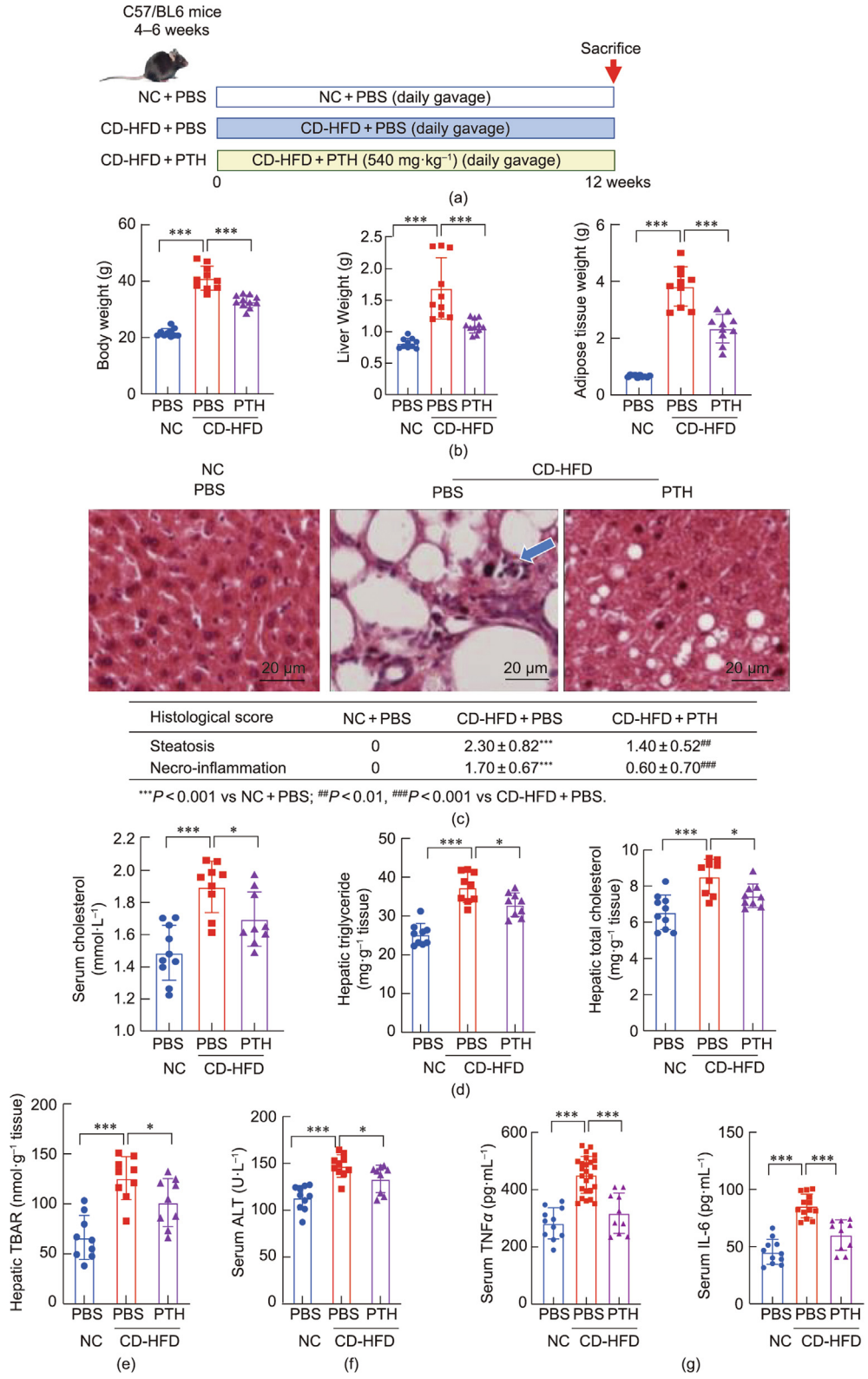

Histological score	NC + PBS	CD-HFD + PBS	CD-HFD + PTH
Steatosis	0	2.30 ± 0.82***	1.40 ± 0.52##
Necro-inflammation	0	1.70 ± 0.67***	0.60 ± 0.70###

***P < 0.001 vs NC + PBS; ##P < 0.01, ###P < 0.001 vs CD-HFD + PBS.

Fig. 2. PTH prevents the development of CD-HFD-induced steatohepatitis. (a) Experimental design for mice fed with NC or CD-HFD supplemented with PTH or PBS control. (b) CD-HFD increased body weight, liver weight, and adipose weight, which were ameliorated by PTH supplement. (c) Representative H&E staining (the arrow indicates inflammatory cells) from liver sections of mice fed with NC or CD-HFD with or without PTH supplementation. Histological scores of steatosis and inflammation were determined. The scale bar represents 20 μm. (d) Serum triglyceride, hepatic triglyceride, and hepatic total cholesterol levels; (e) hepatic TBARs; (f) serum ALT; and (g) serum TNFα and IL-6 levels in mice fed with NC or CD-HFD with or without PTH supplementation. *P < 0.05, **P < 0.01, ***P < 0.001.

We established a third NASH mouse model to investigate whether PTH could suppress steatohepatitis development in different stages by feeding C57BL/6 mice with an MCD diet for 10 days or 4 weeks, with or without PTH (Fig. 3(a)). The MCD diet significantly induced weight loss, while PTH administration further decreased body weight (Fig. S1 in Appendix A). PTH protected mice from MCD diet-induced steatohepatitis, with significantly reduced liver steatosis ($P < 0.05$ for 10 days on an MCD diet; $P < 0.01$ for 4 weeks on an MCD diet) and inflammation ($P < 0.05$ for 10 days on an MCD diet; $P < 0.01$ for 4 weeks on an MCD diet), regardless of the duration of MCD diet feeding (Fig. 3(b)). Consistently, hepatic triglycerides (both $P < 0.001$) and lipid peroxidation ($P < 0.001$ for 10 days on an MCD diet; $P < 0.01$ for 4 weeks on an MCD diet) were significantly decreased in PTH-supplemented mice with 10 days or 4 weeks of feeding on an MCD diet, compared with those without PTH (Fig. 3(c)). Liver injury was also ameliorated in PTH-supplemented mice with 10 days or 4 weeks of feeding on an MCD diet, as evidenced by decreased serum levels of ALT and AST (all $P < 0.001$) (Fig. 3(d)). The increased serum TNFα and IL-6 levels were reduced by the PTH in the 4-week MCD diet-fed mice (Fig. S2 in Appendix A). Consistent with the findings from 10-day and 4-week MCD diet-fed mice, PTH administration for 5 days to MCD diet-fed mice significantly decreased hepatic triglycerides ($P < 0.001$), lipid peroxidation ($P < 0.001$), serum ALT ($P < 0.001$), and AST levels ($P < 0.001$) (Fig. S3 in Appendix A). Taken together, our results from multiple NASH mouse models revealed the preventive effect of PTH against the development of diet-induced steatohepatitis.

3.3. PTH has a therapeutic effect in established steatohepatitis

After confirming the preventive effect of PTH, we next explored whether PTH had therapeutic effects against steatohepatitis. Steatohepatitis was developed in mice after feeding with an MCD diet for 3 weeks; these MCD diet-fed mice then received either PTH treatment or vehicle controls for 10 days (Fig. 4(a)). Histological examination of liver sections showed significantly reduced lipid accumulation and inflammatory cell infiltration in the MCD diet-fed mice with 10 days of PTH treatment, compared with the vehicle controls (both $P < 0.001$) (Fig. 4(b)). PTH treatment also significantly decreased hepatic total cholesterol ($P < 0.01$), triglycerides ($P < 0.01$), lipid peroxidation ($P < 0.001$) (Fig. 4(c)), and serum levels of ALT ($P < 0.01$) and AST ($P < 0.001$) (Fig. 4(d)), indicating the marked alleviation of MCD diet-induced liver injury by PTH treatment. These results thus show the therapeutic potential of PTH on steatohepatitis.

3.4. PTH restores the gut microbiota in mice with steatohepatitis

We profiled the gut microbiota in fecal samples of HFHC diet-fed mice with or without PTH and in NC-fed mice by means of shotgun metagenomic sequencing. Principal component analysis (PCoA) revealed distinct microbial communities among the three groups of HFHC diet-fed mice with PTH, HFHC diet-fed with PBS, and NC-fed mice with PBS (Fig. 5(a)). Significantly lower bacterial diversity (Chao1 index) was observed in the HFHC diet-fed mice compared with the control mice ($P < 0.0001$), while PTH supplementation was found to restore bacterial diversity in the HFHC diet-fed mice ($P < 0.05$) (Fig. 5(b)). The compositions of the fecal bacteria communities of the three groups are shown in Fig. 5(c).

We then used the ternary plot method to identify bacteria associated with PTH treatment at the genus level (Fig. 5(d)). *Lactobacillus*—a genus including many probiotic species that ameliorate NASH progression [18]—was found to be depleted in HFHC diet-fed mice, whereas PTH restored the abundance of *Lactobacillus* back to a level similar to that found in the control mice (Fig. 5(d)). Examination of the microbiota at the species level identified a consortium of bacteria that were significantly enriched by PTH (Fig. 5(e)). The majority of PTH-enriched bacteria were probiotics, including *Lactobacillus* (e.g., *L. acidophilus* and *Lactobacillus plantarum* (*L. plantarum*)), *Lactococcus (e.g., Lactococcus lactis)*, and *Bacillus* (e.g., *Bacillus subtilis*) (Fig. 5(e)). On the other hand, the abundances of several pathogenic bacteria from *Citrobacter* and *Pseudomonas* [19] were decreased by PTH (Fig. 5(e)). Increased abundances of *L. acidophilus* ($P < 0.0001$) and *Lactococcus lactis* ($P < 0.001$) were also found in the stool of the NC-fed mice with PTH administration (Fig. 5(f)). Collectively, our metagenomic analysis revealed that PTH restored the gut microbiota in mice with steatohepatitis by inducing the enrichment of probiotics.

3.5. L. acidophilus protects against steatohepatitis

We next evaluated the effect of enriched probiotic *L. acidophilus* in PTH-prevented NASH. MCD diet-fed mice were gavaged with *L. acidophilus*, *E. coli*, or PBS for 10 consecutive days (Fig. 5(g)). *L. acidophilus*-gavaged mice showed greatly improved liver histology, with reduced steatosis and inflammatory cell infiltration compared with mice gavaged with *E. coli* or PBS (Fig. 5(g)). Accordingly, the liver-to-body weight ratio was significantly decreased by *L. acidophilus* (Fig. 5(g)). These results clearly show that *L. acidophilus* suppressed steatohepatitis development in mice.

3.6. PTH restores gut barrier function in mice

Gut barrier dysfunction driven by microbial dysbiosis is a prerequisite for steatohepatitis development [20]. To test whether the gut barrier contributes to the anti-steatohepatitis effects of PTH, we examined the paracellular permeability in mice colon by measuring the serum LPS level. Serum LPS concentration was elevated in mice fed with an HFHC diet, a CD-HFD, and an MCD diet, compared with NC or corresponding control diet-fed mice (all $P < 0.001$) (Fig. 6(a)), confirming the impaired gut barrier function in multiple NASH mouse models. PTH significantly decreased serum LPS levels in all diet-induced NASH mouse models, compared with mice without PTH ($P < 0.05$ for CD-HFD-fed mice; $P < 0.001$ for HFHC diet-fed and MCD diet-fed mice) (Fig. 6(a)). MCD diet-fed mice supplemented with PTH showed a significant reduction in intestinal permeability according to FITC-dextran assay ($P < 0.05$) (Fig. 6(b)), implying that gut barrier function was restored upon PTH administration. Consistently, the expression of E-cadherin—a cell adhesion molecule and marker of gut barrier integrity—was significantly increased in HFHC diet-fed ($P < 0.01$), MCD diet-fed ($P < 0.05$), and CD-HFD-fed ($P < 0.05$) mice with PTH treatment (Fig. 6(c)). Moreover, 10 days of PTH treatment after the onset of MCD diet-induced steatohepatitis reduced the serum LPS level in mice, compared with the PBS controls ($P < 0.001$) (Fig. 6(d)). Taken together, these results indicate that PTH alleviates NASH development at least in part by restoring a functional gut barrier.

3.7. PTH influences the bile acid metabolism in the portal vein of mice

Gut microbial dysbiosis impairs the gut–liver axis, leading to unrestrained transfer of metabolites from the intestines into the liver. Some of these translocated metabolites can be harmful, which may cause liver injury and contribute to NASH development [12]. To reveal the metabolomic phenotypes associated with PTH treatment, we performed untargeted metabolomics on the portal vein blood of mice fed with NC, an HFHC diet, or an HFHC diet with PTH. PCoA showed a marked disparity in the metabolites in the portal vein among the three groups of mice (Fig. 7(a)). Nineteen metabolites were found to be significantly enriched in the portal

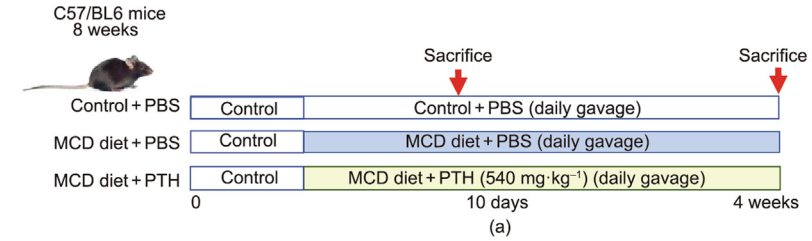

(a)

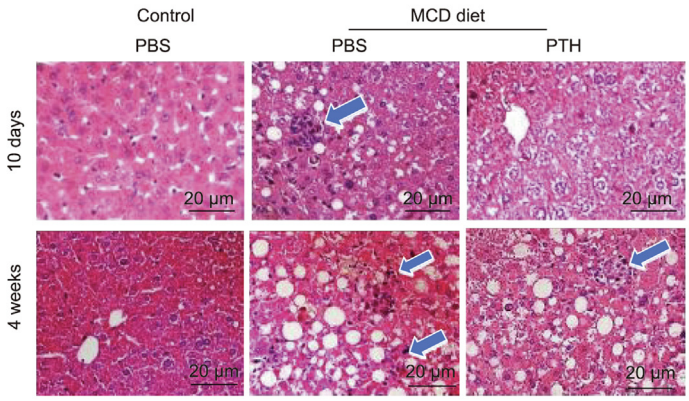

Histological score	10 days			4 weeks		
	Control + PBS	MCD diet + PBS	MCD diet + PTH	Control + PBS	MCD diet + PBS	MCD diet + PTH
Steatosis	0	1.60 ± 1.14**	0.20 ± 0.45#	0	2.50 ± 0.53***	1.88 ± 0.35##
Necro-inflammation	0	1.20 ± 0.84*	0.20 ± 0.45#	0	2.34 ± 0.52***	1.56 ± 0.53##

*P < 0.05, **P < 0.01, ***P < 0.001 vs Control + PBS; #P < 0.05, ##P < 0.01 vs MCD diet + PBS.

(b)

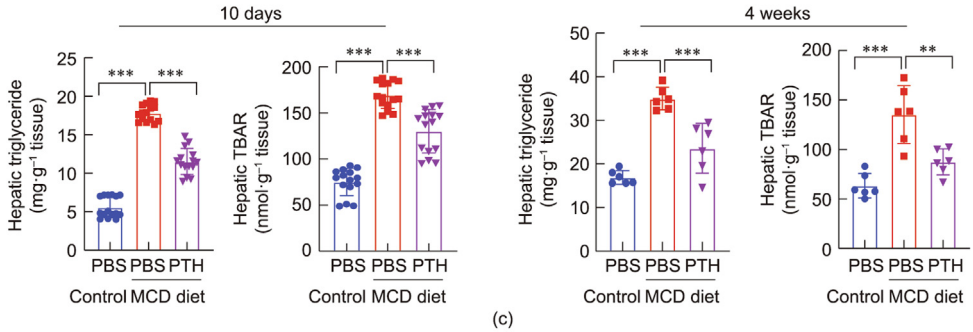

(c)

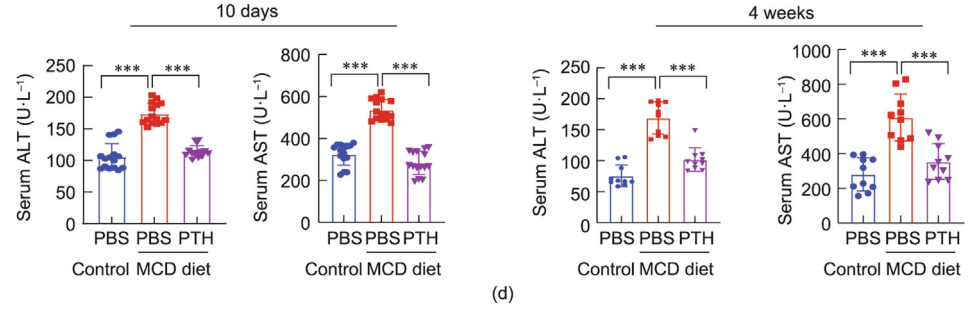

(d)

Fig. 3. PTH prevents the development of MCD diet-induced steatohepatitis. (a) Experimental design for mice fed with control or an MCD diet with or without PTH supplementation. (b) Representative H&E staining (arrows indicate inflammatory cells) from liver sections of mice fed with control or an MCD diet with or without PTH supplementation for 10 days and 4 weeks. Histological scores of steatosis and inflammation were determined. The scale bar represents 20 μm. (c) Hepatic triglyceride and hepatic TBARs in mice fed with an MCD diet with or without PTH for 10 days and 4 weeks. (d) Serum ALT and AST in mice fed with an MCD diet with or without PTH administration for 10 days and 4 weeks. *P < 0.05, **P < 0.01, ***P < 0.001.

vein of HFHC diet-fed mice with PTH, compared with those without PTH (Fig. 7(b)). In contrast, 21 metabolites were depleted in the portal vein of PTH-supplemented HFHC diet-fed mice. To understand the functional characteristics of the enriched metabolites, we conducted a pathway enrichment analysis and found that bile acid biosynthesis was one of the top altered pathways among the portal vein metabolites in PTH-treated mice (Fig. 7(c)). Further examination of the portal vein metabolites showed that serum levels of conjugated bile acids including tauroursodeoxycholic acid (TUDCA; P < 0.001), taurodeoxycholic acid (TDCA; P < 0.01), glycocholic acid (GCA; P < 0.01), taurocholic acid (TCA; P < 0.001), and chenodeoxycholic acid (CDCA; P < 0.05) were significantly

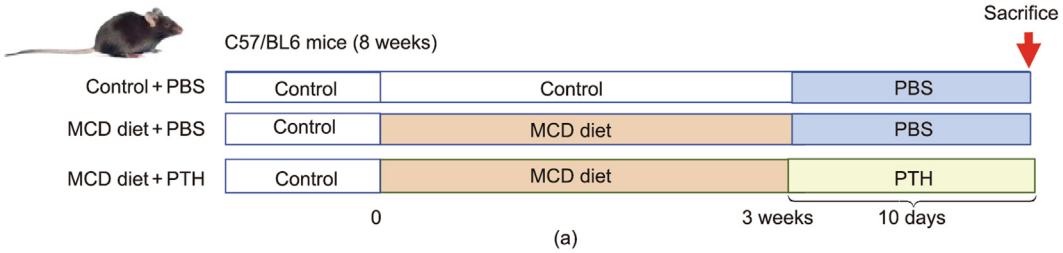

(a)

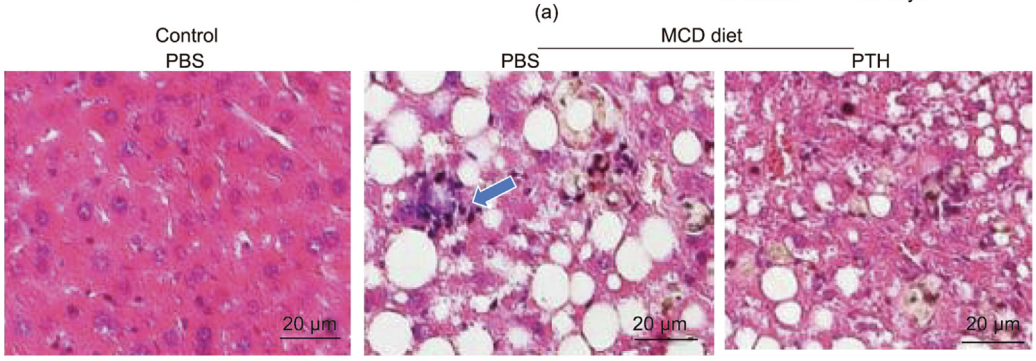

Histological score	Control + PBS	MCD diet + PBS	MCD diet + PTH
Steatosis	0	3.00 ± 0***	2.00 ± 0.47###
Necro-inflammation	0	3.00 ± 0***	2.00 ± 0.67###

***P < 0.001 vs Control + PBS; ###P < 0.001 vs MCD diet + PBS.

(b)

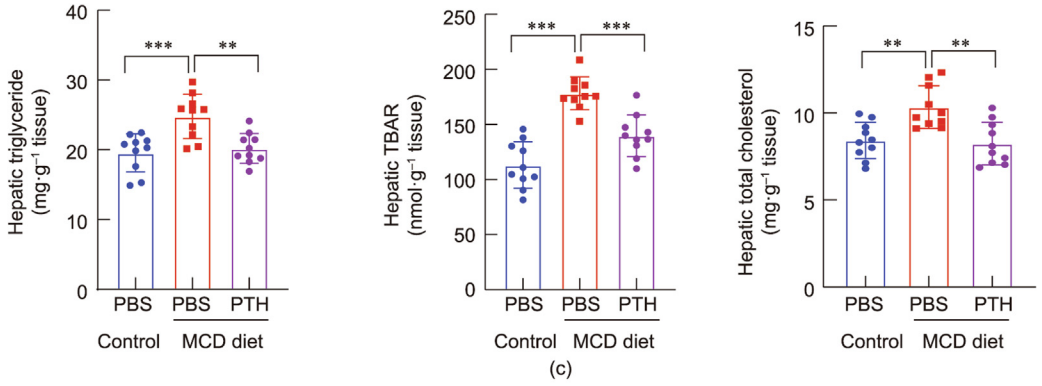

(c)

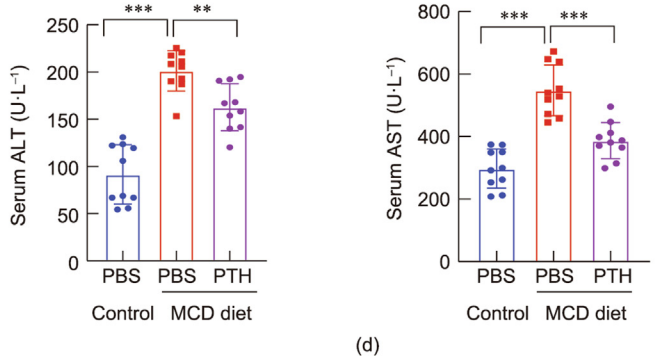

(d)

Fig. 4. PTH has therapeutic effects against steatohepatitis. (a) Experimental design for mice fed with control or an MCD diet treated with PBS or PTH; (b) Representative H&E staining (the arrow indicates inflammatory cells) from liver sections of mice fed with control or an MCD diet treated with PTH or PBS control for 10 days after NASH establishment. Histological scores of steatosis and inflammation were determined. The scale bar represents 20 μm. (c) Hepatic total cholesterol, triglyceride, and TBARs in mice treated with PTH. (d) Serum ALT and AST in mice fed with an MCD diet treated with PTH or PBS control for 10 days. *P < 0.05, **P < 0.01, ***P < 0.001.

upregulated in PTH-supplemented HFHC diet-fed mice, compared with those without PTH (Fig. 7(d) and Fig. S4 in Appendix A). Moreover, the ratio of deoxycholic acid (DCA) to CDCA in the portal vein—which is a marker of human NASH [12]—was significantly decreased in HFHC diet-fed mice administrated with PTH (P < 0.05) (Fig. 7(e)).

Conjugated bile acids play an important role in NASH by binding with farnesoid X receptor (FXR) in the intestine to regulate the production of hormone fibroblast growth factor 15 (FGF15), which is secreted into the liver to reduce bile acid synthesis [21]. Given the upregulation of conjugated bile acids after PTH administration, we chose to examine the expression of *Fxr* and *Fgf15* in the

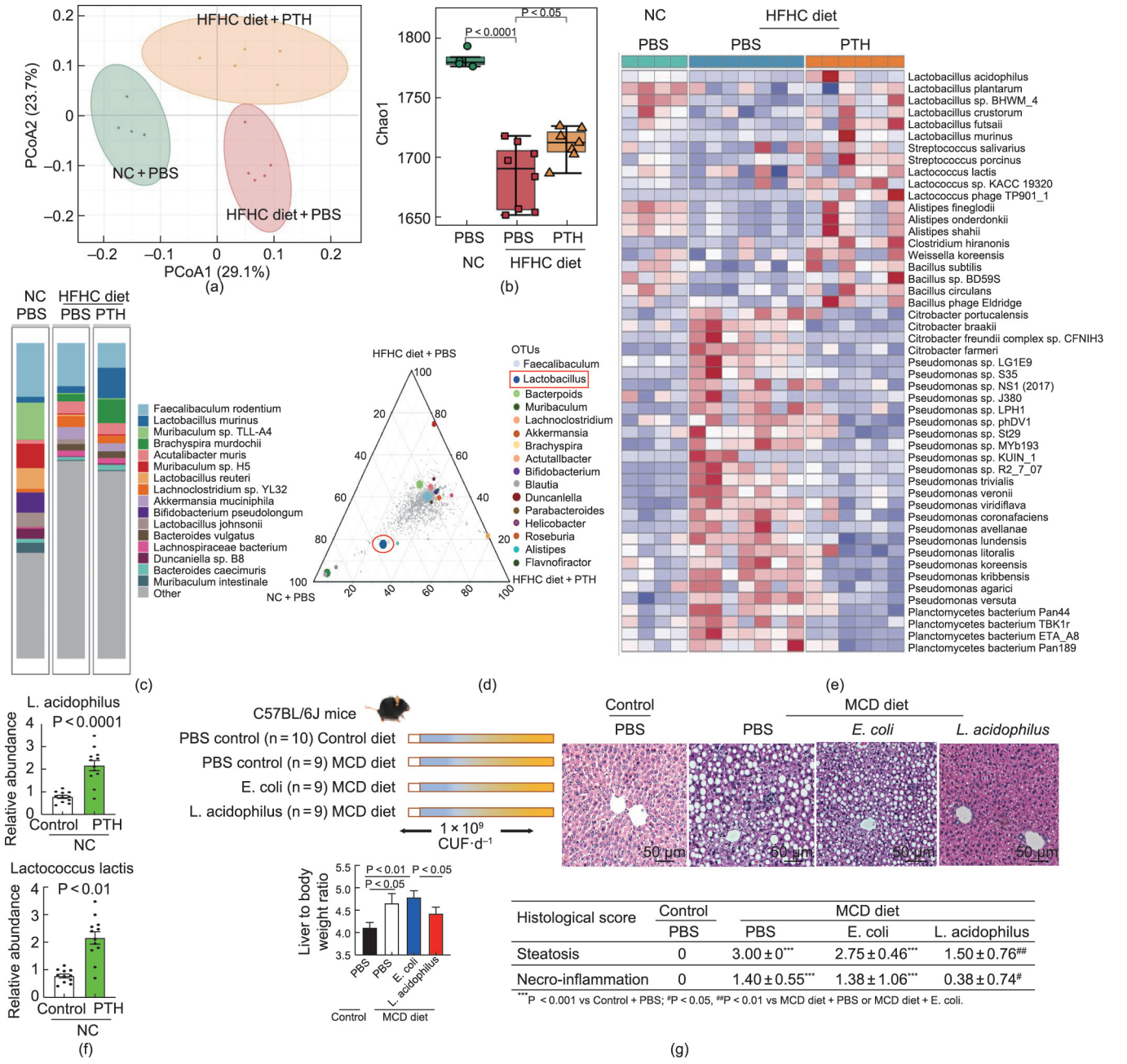

Histological score	Control	MCD diet		
	PBS	PBS	E. coli	L. acidophilus
Steatosis	0	3.00 ± 0***	2.75 ± 0.46***	1.50 ± 0.76##
Necro-inflammation	0	1.40 ± 0.55***	1.38 ± 1.06***	0.38 ± 0.74#

***P < 0.001 vs Control + PBS; #P < 0.05, ##P < 0.01 vs MCD diet + PBS or MCD diet + E. coli.

Fig. 5. PTH ameliorates gut microbiota dysbiosis in mice with steatohepatitis. (a) Unsupervised PCoA of gut microbiota in NC-fed or HFHC diet-fed mice treated with PTH or PBS control. (b) Chao 1 diversity in NC-fed or HFHC diet-fed mice treated with PTH or PBS control. (c) Abundance of differential bacteria in NC-fed or HFHC diet-fed mice supplemented with PTH or PBS control. (d) Ternary plot of the gut microbiota in NC-fed or HFHC diet-fed mice supplemented with PTH or PBS control. OTUs: operational taxonomic units. (e) Heatmap of the gut microbiota in NC-fed or HFHC diet-fed mice supplemented with PTH or PBS control. (f) Abundance of *L. acidophilus* and *Lactococcus lactis* in NC-fed mice treated with PTH for 3 months. (g) *L. acidophilus* was gavaged to control or MCD diet-fed mice for 10 days; representative H&E-stained histological images of liver tissues are shown here. Histological scores of steatosis and inflammation were calculated. *L. acidophilus* administration reduced the liver-to-body weight ratio and hepatic lipid peroxidation in MCD diet-fed mice.

intestine of HFHC diet-fed mice. Our results showed that intestine *Fxr* and *Fgf15* mRNA levels were significantly decreased by PTH supplementation (both $P < 0.01$) (Fig. 7(f)). In contrast, hepatic mRNA expression of bile acids biosynthesis including cytochrome P450 (*Cyp7a1*, *Cyp7b1*, and *Cyp27a1*) was significantly increased in PTH-supplemented mice, compared with mice without PTH ($P < 0.01$) (Fig. 7(f)). Taken together, our results suggest that PTH mainly upregulates conjugated bile acids and reduces the secretion of intestinal Fgf15, thereby at least partially suppressing NASH development.

We also investigated the chemical identities of PTH by means of LC-MS. The main compounds in the formula of PTH include ginsenoside (ginsenoside Rg1, Rg2, Rg5, Rf, Rb1, Rb3, and F2) and bile acids (CA, CDCA, hyodeoxycholic acid, gentisic acid, and lithocholic acid). The relevant MS/MS spectra of the main compounds are provided in Fig. S5 in Appendix A.

3.8. An intact gut microbiota is essential in PTH's amelioration of steatohepatitis

To evaluate the role of the gut microbiota in PTH-induced NASH prevention, an antibiotics cocktail was used to deplete the gut microbiota in HFHC diet-fed or MCD diet-fed mice with or without PTH supplementation (Figs. S6 and S7 in Appendix A).

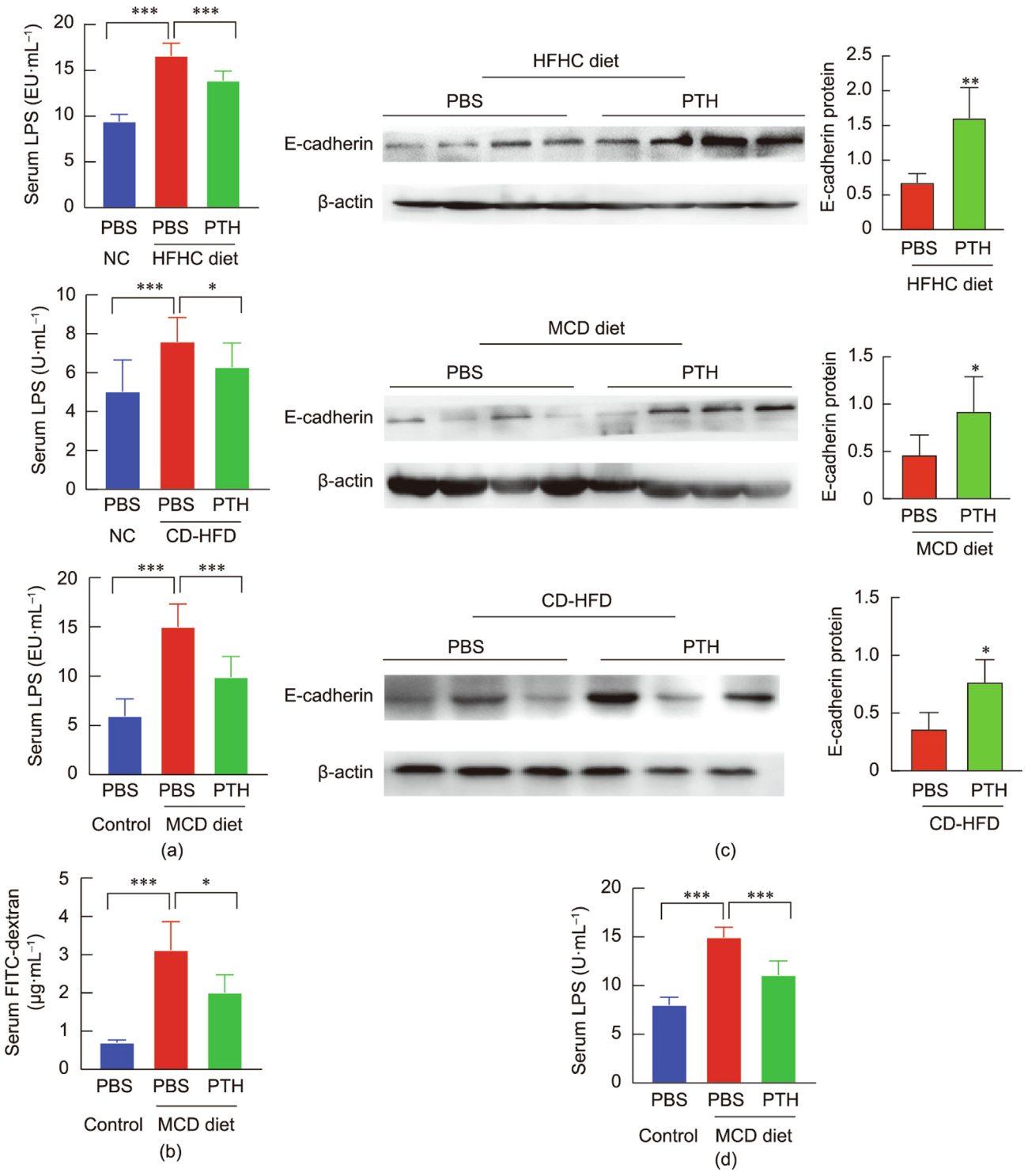

Fig. 6. PTH restores gut barrier function. (a) Serum LPS levels in HFHC diet-, CD-HFD-, and MCD diet-induced steatohepatitis supplemented with PTH or PBS control. (b) Serum FITC-dextran in MCD diet-induced steatohepatitis supplemented with PTH or PBS control for 10 days. (c) Western blot analysis of E-cadherin in the colon of mice fed with an HFHC diet or MCD diet supplemented with PTH or PBS control. (d) Serum LPS levels in MCD diet-induced steatohepatitis treated with PTH or PBS control for 10 days. EU: endotoxin units. $^{*}P < 0.05$, $^{**}P < 0.01$, $^{***}P < 0.001$.

We found that PTH administration did not ameliorate steatohepatitis development in microbiota-depleted HFHC diet-fed mice, since these mice exhibited levels of steatosis, inflammation, and hepatic lipid peroxidation similar to those of microbiota-depleted HFHC diet-fed mice without PTH (Fig. S6). PTH also consistently failed to suppress steatohepatitis development in microbiota-depleted MCD diet-fed mice, since these mice exhibited levels of serum ALT, AST, hepatic triglyceride, and lipid peroxidation similar to those of mice without PTH treatment (Fig. S7). The probiotics enriched by PTH were eliminated by antibiotics administration (Fig. S8 in Appendix A). These findings clearly illustrate that the gut microbiota is essential for PTH to exhibit its anti-steatohepatitis effects against NASH development.

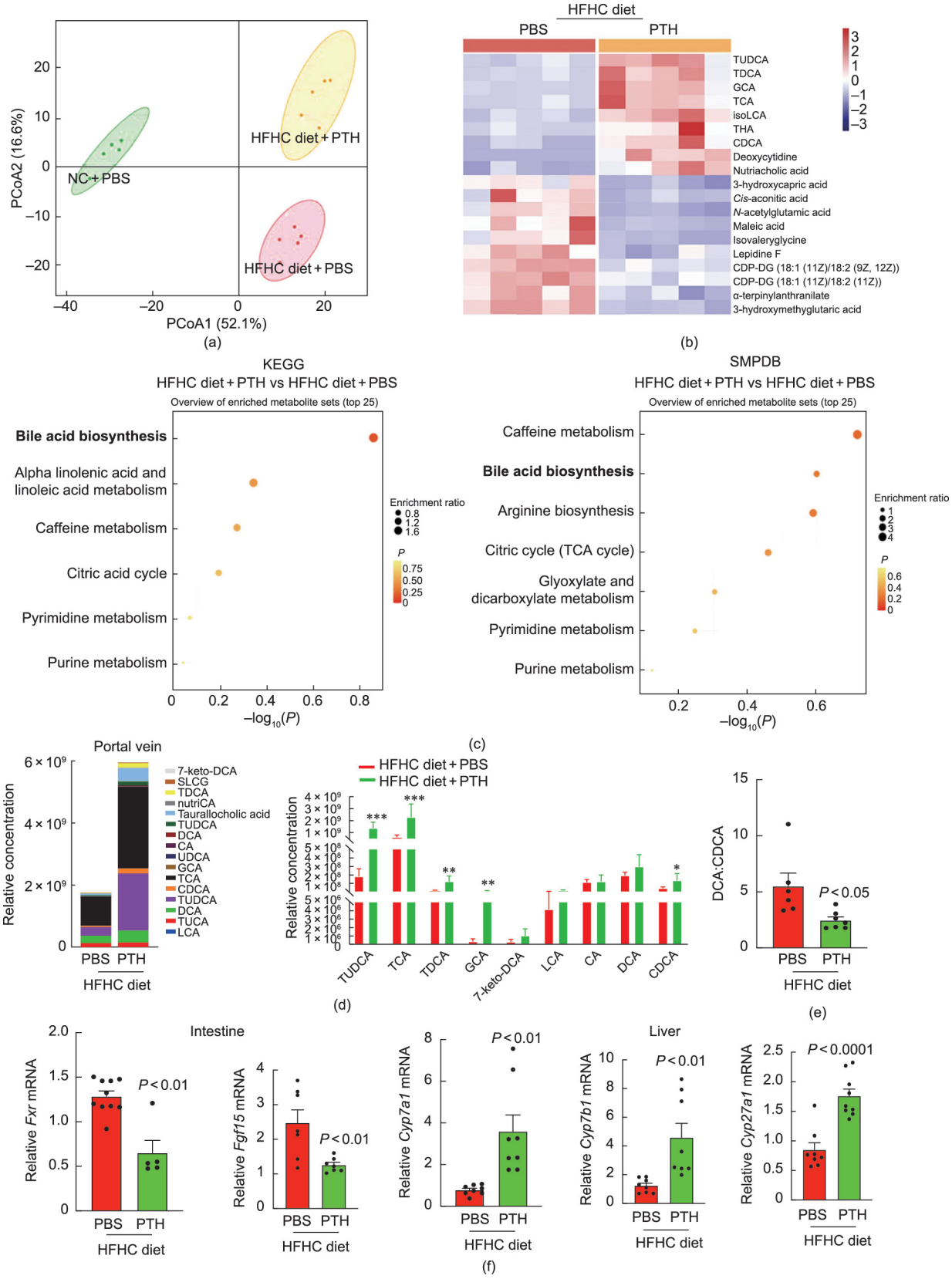

Fig. 7. PTH influences the composition of bile acid metabolism in the HFHC diet mice model. (a) Untargeted metabolomics was performed in the portal vein of mice fed with NC, an HFHC diet, or an HFHC diet with PTH administration. PCoA showed the marked disparity of metabolites among three groups. (b) Heatmap of differential metabolites in HFHC diet-fed mice with PTH or PBS control supplementation. (c) Kyoto Encyclopedia of Genes and Genomes (KEGG) and The Small Molecule Pathway Database (SMPDB) pathway enrichment analysis in the portal vein metabolites of PTH-supplemented mice. (d) Altered bile acids in the portal vein of mice fed with an HFHC diet with PTH or PBS control supplementation. (e) Ratio of DCA to CDCA in the portal vein of HFHC diet-fed mice with PTH or PBS control supplementation. (f) Intestine *Fxr* and *Fgf15* mRNA levels, liver *Cyp7a1*, *Cyp7b1*, and *Cyp27a1* mRNA levels in HFHC diet-fed mice supplemented with PTH or PBS control. TUDCA: tauroursodeoxycholic acid; TDCA: taurodeoxycholic acid; GCA: glycocholic acid; TCA: taurocholic acid; isoLCA: isolithocholic acid; THA: tetracosahexaenoic acid; CDCA: chenodeoxycholic acid; GDP-DG: cytidine diphosphate diacylglycerol; 7-keto-DCA, 7-Ketodeoxycholic acid; SLCG, Sulfolithocholylglycine; nutriCA, Nutriacholic acid; CA: cholic acid; UDCA: Ursodeoxycholic acid; DCA: deoxycholic acid; TUCA, Tauroursocholic acid; LCA: lithocholic acid. $^{*}P < 0.05$, $^{**}P < 0.01$, $^{***}P < 0.001$.

4. Discussion

PTH is known for its anti-inflammatory effects, yet its efficacy against NASH has not been investigated. In this study, our results showed that PTH significantly prevented the development of diet-induced steatohepatitis in multiple mouse models. Moreover, PTH reversed the established NASH, indicating its therapeutic role in NASH. PTH supplementation improved liver histology, reduced hepatic triglyceride, cholesterol, and lipid peroxide, and decreased serum ALT and AST levels, thereby contributing to the prevention and regression of mice steatohepatitis. PTH has been widely used to treat liver disease for 600 years [22]. Preclinical studies have shown that PTH attenuates carbon tetrachloride-induced liver injury, inflammation, and fibrosis [23,24], and inhibits the proliferation of liver cancer cell lines [25]. Our study therefore extends the notion that PTH can act as a novel prophylactic and therapeutic drug for NASH, a highly prevalent and progressive disease with unmet clinical need.

The association of the gut microbiota with liver diseases has been increasingly acknowledged. Gut microbiome dysbiosis with lower microbial diversity has been reported in both human NASH [26,27] and mouse NASH models [9]. However, human NASH patients showed increased abundance of *Bacteroides* [28] and *Proteobacteria* [29], while *Enterobacteriales* [30] was enriched in mouse NASH models. Although the altered bacteria are different between human and mouse NASH, modulation of the gut microbiome by probiotics (*Lactobacillus* and *Bifidobacterium*) or fecal microbiome transplantation was found to ameliorate NASH in both humans and mice [11,31]. Our metagenomic analysis revealed enrichment of the beneficial probiotics *Lactobacillus*, *Alistipes*, and *Bacillus* after PTH treatment. In particular, *L. acidophilus* and *L. plantarum*—two *Lactobacillus* species that have been widely commercialized—were found to be enriched in PTH-treated mice with ameliorated NASH. A pilot clinical study performed in our institution showed that a probiotic formula containing *L. acidophilus* and *L. plantarum* reduced liver fat and ameliorated liver injury in NASH patients [32]. We confirmed that the enriched *L. acidophilus* prevented steatohepatitis in MCD diet-fed mice. *Lactococcus lactis*, a beneficial microbe that suppresses hepatis steatosis and inflammation [33], was also found to be enriched in the mice administered with PTH. The probiotic *Bacillus subtilis* ameliorates liver inflammation, improves gut barrier function, and modulates gut microbiota in mice with NAFLD [34]. We previously reported that a high intake of dietary cholesterol induces microbial dysbiosis in mice, and that the dysbiotic microbiota then contributes to the pathogenesis of NASH and its related hepatocellular carcinoma [9]. Several TCMs have been shown to ameliorate human NAFLD effectively by modulating the gut microbiota [35]. Collectively, our study suggests that PTH suppresses NASH by alleviating dysbiosis and enriching probiotics.

Gut dysbiosis promotes liver pathologies in many different ways, particularly by damaging the gut barrier, with markedly increased intestinal permeability [36]. In general, dysbiotic microbiota impair the gut barrier, thereby allowing the translocation of more pathogenic bacteria and their derived toxic metabolites to the liver through portal vein circulation [36]. Our findings illustrate the occurrence of gut barrier dysfunction in mice with diet-induced steatohepatitis. Notably, PTH treatment greatly restored the impaired gut barrier, as indicated by increased intestinal permeability, reduced serum endotoxin LPS level, and increased expression of tight-junction protein E-cadherin. The gut barrier restored by PTH may prevent the translocation of pathogenic bacteria and toxic metabolites into the liver, thereby protecting mice from liver injury. Indeed, pharmacological drugs that improve the gut barrier can prevent and treat NASH [20]. Our results suggest that PTH can act as a drug to protect against gut barrier disruption and suppress NASH development.

The metabolites produced by gut microbes are important in the development of steatohepatitis, as toxic metabolites can induce liver damage through the gut–liver axis [11]. In this study, our metabolomic analysis revealed the enrichment of conjugated bile acids, including TUDCA, TCA, TDCA and GCA in PTH-treated mice. Bile acids are crucial metabolites that modulate lipid metabolism [37]. TUDCA attenuates diet-induced hepatic steatosis, inflammation, obesity, and insulin resistance by modulating the gut microbiota and improving gut barrier function [38]. TUDCA also suppresses intestinal FXR–FGF15 signaling, which mediates activation of the cytochrome P450 family enzyme in hepatocytes and the metabolism of bile acids [39]. In our experiments, intestinal *Fxr–Fgf15* was suppressed, whereas hepatic genes for bile acid synthesis, including *Cyp7a1*, *Cyp7b1*, and *Cyp27a1*, were upregulated. Therefore, our results suggest that PTH inhibits the intestinal FXR signaling pathway to promote bile acid synthesis in the liver, thereby suppressing NASH.

5. Conclusions

This study demonstrates, for the first time, that PTH could be an effective prophylactic and therapeutic against steatohepatitis. Mechanistically, PTH modulates the gut microbiota and restores the functions of the gut barrier and the altered gut metabolites, thereby alleviating the development and progression of NASH through the gut–liver axis.

Authors' contribution

Xianyi Zeng and Xiang Zhang performed experiments, analyzed the data, and drafted the manuscript; Hao Su, Hongyan Gou, and Yan Li performed experiments; Harry Cheuk-Hay Lau revised the manuscript; Xiaoxu Hu and Ziheng Huang performed the bioinformatic analysis; Jun Yu designed and supervised the study and wrote the paper.

Compliance with ethics guidelines

Xianyi Zeng, Xiang Zhang, Hao Su, Hongyan Gou, Harry Cheuk-Hay Lau, Xiaoxu Hu, Ziheng Huang, Yan Li, and Jun Yu declare that they have no conflict of interest or financial conflicts to disclose.

Acknowledgments

This work was supported by the National Natural Science Foundation of China (82103355 and 82222901); Research Grants Council-General Research Fund (RGC-GRF; 14117422); Health and Medical Research Fund, Hong Kong (08191336); and Vice-Chancellor's Discretionary Fund CUHK.

Appendix A. Supplementary material

Supplementary data to this article can be found online at https://doi.org/10.1016/j.eng.2022.10.010.

References

[1] Yip TC, Lee HW, Chan WK, Wong GL, Wong VW. Asian perspective on NAFLD-associated HCC. J Hepatol 2022;76(3):726–34.
[2] Loomba R, Friedman SL, Shulman GI. Mechanisms and disease consequences of nonalcoholic fatty liver disease. Cell 2021;184(10):2537–64.
[3] Wong VW, Chitturi S, Wong GL, Yu J, Chan HL, Farrell GC. Pathogenesis and novel treatment options for non-alcoholic steatohepatitis. Lancet Gastroenterol Hepatol 2016;1(1):56–67.

[4] Francque SM, Bedossa P, Ratziu V, Anstee QM, Bugianesi E, Sanyal AJ, et al.; NATIVE Study Group. A randomized, controlled trial of the Pan-PPAR agonist lanifibranor in NASH. N Engl J Med 2021;385(17):1547–58.
[5] Shi T, Wu Li, Ma W, Ju L, Bai M, Chen X, et al. Nonalcoholic fatty liver disease: pathogenesis and treatment in traditional Chinese medicine and western medicine. Evid Based Complement Alternat Med 2020;2020:1–16.
[6] Huang L, Zhang Y, Zhang X, Chen X, Wang Y, Lu J, et al. Therapeutic potential of Pien-Tze-Huang: a review on its chemical composition, pharmacology, and clinical application. Molecules 2019;24(18):3274.
[7] Lau JK, Zhang X, Yu J. Animal models of non-alcoholic fatty liver disease: current perspectives and recent advances. J Pathol 2017;241(1):36–44.
[8] Wolf M, Adili A, Piotrowitz K, Abdullah Z, Boege Y, Stemmer K, et al. Metabolic activation of intrahepatic $CD8^+$ T cells and NKT cells causes nonalcoholic steatohepatitis and liver cancer via cross-talk with hepatocytes. Cancer Cell 2014;26(4):549–64.
[9] Zhang X, Coker OO, Chu ESH, Fu K, Lau HCH, Wang YX, et al. Dietary cholesterol drives fatty liver-associated liver cancer by modulating gut microbiota and metabolites. Gut 2021;70(4):761–74.
[10] Carter JK, Bhattacharya D, Borgerding JN, Fiel MI, Faith JJ, Friedman SL. Modeling dysbiosis of human NASH in mice: loss of gut microbiome diversity and overgrowth of Erysipelotrichales. PLoS One 2021;16(1):e0244763.
[11] Pan Y, Zhang X. Diet and gut microbiome in fatty liver and its associated liver cancer. J Gastroenterol Hepatol 2022;37(1):7–14.
[12] Chu H, Duan Y, Yang L, Schnabl B. Small metabolites, possible big changes: a microbiota-centered view of non-alcoholic fatty liver disease. Gut 2019;68(2):359–70.
[13] Chang CJ, Lin CS, Lu CC, Martel J, Ko YF, Ojcius DM, et al. Ganoderma lucidum reduces obesity in mice by modulating the composition of the gut microbiota. Nat Commun 2015;6(1):7489.
[14] Li Y, Ji X, Wu H, Li X, Zhang H, Tang D. Mechanisms of traditional Chinese medicine in modulating gut microbiota metabolites-mediated lipid metabolism. J Ethnopharmacol 2021;278:114207.
[15] Zhang X, Fan L, Wu J, Xu H, Leung WY, Fu K, et al. Macrophage p38α promotes nutritional steatohepatitis through M1 polarization. J Hepatol 2019;71(1):163–74.
[16] Yang J, Wei H, Zhou Y, Szeto C-H, Li C, Lin Y, et al. High-fat diet promotes colorectal tumorigenesis through modulating gut microbiota and metabolites. Gastroenterology 2022;162(1):135–49.e2.
[17] Venkatesh M, Mukherjee S, Wang H, Li H, Sun K, Benechet A, et al. Symbiotic bacterial metabolites regulate gastrointestinal barrier function via the xenobiotic sensor PXR and Toll-like receptor 4. Immunity 2014;41(2):296–310.
[18] Lee NY, Shin MJ, Youn GS, Yoon SJ, Choi YR, Kim HS, et al. *Lactobacillus* attenuates progression of nonalcoholic fatty liver disease by lowering cholesterol and steatosis. Clin Mol Hepatol 2021;27(1):110–24.
[19] Jäger AV, Arias P, Tribulatti MV, Brocco MA, Pepe MV, Kierbel A. The inflammatory response induced by *Pseudomonas aeruginosa* in macrophages enhances apoptotic cell removal. Sci Rep 2021;11(1):2393.
[20] Mouries J, Brescia P, Silvestri A, Spadoni I, Sorribas M, Wiest R, et al. Microbiota-driven gut vascular barrier disruption is a prerequisite for non-alcoholic steatohepatitis development. J Hepatol 2019;71(6):1216–28.
[21] Sinal CJ, Tohkin M, Miyata M, Ward JM, Lambert G, Gonzalez FJ. Targeted disruption of the nuclear receptor FXR/BAR impairs bile acid and lipid homeostasis. Cell 2000;102(6):731–44.
[22] Zhu J, Zhang Di, Wang T, Chen Z, Chen L, Wu H, et al. Target identification of hepatic fibrosis using Pien Tze Huang based on mRNA and lncRNA. Sci Rep 2021;11(1):16980.
[23] Zhao J, Hu H, Wan Y, Zhang Y, Zheng L, Hong Z. Pien Tze Huang Gan Bao ameliorates carbon tetrachloride-induced hepatic injury, oxidative stress and inflammation in rats. Exp Ther Med 2017;13(5):1820–6.
[24] Zheng H, Wang X, Zhang Y, Chen Li, Hua L, Xu W. Pien-Tze-Huang ameliorates hepatic fibrosis via suppressing NF-κB pathway and promoting HSC apoptosis. J Ethnopharmacol 2019;244:111856.
[25] Qi F, Zhou S, Li L, Wei L, Shen A, Liu L, et al. Pien Tze Huang inhibits the growth of hepatocellular carcinoma cells by upregulating miR-16 expression. Oncol Lett 2017;14(6):8132–7.
[26] Shen F, Zheng RD, Sun XQ, Ding WJ, Wang XY, Fan JG. Gut microbiota dysbiosis in patients with non-alcoholic fatty liver disease. Hepatobiliary Pancreat Dis Int 2017;16(4):375–81.
[27] Zhu L, Baker SS, Gill C, Liu W, Alkhouri R, Baker RD, et al. Characterization of gut microbiomes in nonalcoholic steatohepatitis (NASH) patients: a connection between endogenous alcohol and NASH. Hepatology 2013;57(2):601–9.
[28] Boursier J, Mueller O, Barret M, Machado M, Fizanne L, Araujo-Perez F, et al. The severity of nonalcoholic fatty liver disease is associated with gut dysbiosis and shift in the metabolic function of the gut microbiota. Hepatology 2016;63(3):764–75.
[29] Hoyles L, Fernández-Real J-M, Federici M, Serino M, Abbott J, Charpentier J, et al. Molecular phenomics and metagenomics of hepatic steatosis in non-diabetic obese women. Nat Med 2018;24(7):1070–80.
[30] Mujico JR, Baccan GC, Gheorghe A, Díaz LE, Marcos A. Changes in gut microbiota due to supplemented fatty acids in diet-induced obese mice. Br J Nutr 2013;110(4):711–20.
[31] Ebrahimzadeh Leylabadlo H, Ghotaslou R, Samadi Kafil H, Feizabadi MM, Moaddab SY, Farajnia S, et al. Non-alcoholic fatty liver diseases: from role of gut microbiota to microbial-based therapies. Eur J Clin Microbiol Infect Dis 2020;39(4):613–27.
[32] Wong VS, Wong GH, Chim AL, Chu WW, Yeung DW, Li KT, et al. Treatment of nonalcoholic steatohepatitis with probiotics. A proof-of-concept study Ann Hepatol 2013;12(2):256–62.
[33] Naudin CR, Maner-Smith K, Owens JA, Wynn GM, Robinson BS, Matthews JD, et al. *Lactococcus lactis* subspecies cremoris elicits protection against metabolic changes induced by a western-style diet. Gastroenterology 2020;159(2):639–51.e5.
[34] Jiang J, Xiong J, Ni J, Chen C, Wang K. Live combined *B. subtilis* and *E. faecium* alleviate liver inflammation, improve intestinal barrier function, and modulate gut microbiota in mice with non-alcoholic fatty liver disease. Med Sci Monit 2021;27:e931143.
[35] Yang XF, Lu M, You L, Gen H, Yuan L, Tian T, et al. Herbal therapy for ameliorating nonalcoholic fatty liver disease via rebuilding the intestinal microecology. Chin Med 2021;16(1):62.
[36] Song Q, Zhang X. The role of gut–liver axis in gut microbiome dysbiosis associated NAFLD and NAFLD-HCC. Biomedicines 2022;10(3):10.
[37] Jia W, Xie G, Jia W. Bile acid-microbiota crosstalk in gastrointestinal inflammation and carcinogenesis. Nat Rev Gastroenterol Hepatol 2018;15(2):111–28.
[38] Wang W, Zhao J, Gui W, Sun D, Dai H, Xiao Li, et al. Tauroursodeoxycholic acid inhibits intestinal inflammation and barrier disruption in mice with non-alcoholic fatty liver disease. Br J Pharmacol 2018;175(3):469–84.
[39] Huang F, Zheng X, Ma X, Jiang R, Zhou W, Zhou S, et al. Theabrownin from Pu-erh tea attenuates hypercholesterolemia via modulation of gut microbiota and bile acid metabolism. Nat Commun 2019;10(1):4971.